Actin Depolymerization Is Associated with Meiotic Acceleration in Cycloheximide-Treated Ovine Oocytes 1

Authors: German, Sergio D., Lee, Joon-Hee, Campbell, Keith H., Sweetman, Dylan, and Alberio, Ramiro

Source: Biology of Reproduction, 92(4)

Published By: Society for the Study of Reproduction

URL: https://doi.org/10.1095/biolreprod.114.122341

BIOLOGY OF REPRODUCTION (2015) **92**(4):103, 1–9
Published online before print 18 March 2015.
DOI 10.1095/biolreprod.114.122341

Actin Depolymerization Is Associated with Meiotic Acceleration in Cycloheximide-Treated Ovine Oocytes[1]

Sergio D. German,[5] Joon-Hee Lee,[6,7] Keith H. Campbell,[4,5] Dylan Sweetman,[3,5] and Ramiro Alberio[2,5]

[5]*Division of Animal Sciences, School of Biosciences, University of Nottingham, Sutton Bonington Campus, Loughborough, United Kingdom*
[6]*Department of Animal Bioscience, College of Agriculture and Life Sciences, Gyeongsang National University, Jinju, Republic of Korea*
[7]*Institute of Agriculture & Life Science, College of Agriculture and Life Sciences, Gyeongsang National University, Jinju, Republic of Korea*

ABSTRACT

Oocytes treated with the protein synthesis inhibitor cycloheximide (CHX) arrest at the germinal vesicle (GV) stage and undergo accelerated GV breakdown (GVBD) after CHX is removed. However, little is known about the underlying mechanism of accelerated meiotic maturation. Here, we investigated this mechanism and found that oocytes released from CHX arrest have higher amounts of cyclin B1 (CCNB1) and phosphorylated mitogen-activated protein kinase (pMAPK) proteins. Increased levels of these factors were not associated with mRNA polyadenylation or increased transcription rates of *CCNB1* and *MOS* (Moloney murine sarcoma viral oncogene homolog) during CHX arrest. We found that treatment of CHX-arrested oocytes with the actin filament-stabilizing agent Jasplakinolide (Jasp) delayed GVBD following release from CHX arrest and that this was correlated with reduced maturation-promoting factor (MPF) activity. These results suggest that *CCNB1* mRNAs released from actin filaments during CHX arrest increase *CCNB1* transcripts available for translation after release from CHX arrest, leading to the precocious activation of MPF and accelerated meiotic progression.

actin depolymerization, cyclin B1, cycloheximide, cytoskeleton, GVBD, IVM, meiotic arrest, meiotic maturation, oocyte maturation, polyadenylation, protein kinases, RNA granules

INTRODUCTION

Fully grown, immature mammalian oocytes are arrested at the germinal vesicle (GV) stage but resume meiosis under the influence of maturation-promoting factor (MPF) and mitogen-activated protein kinase (MAPK). MPF is a complex composed of the regulatory subunit cyclin B1 (CCNB1) and the catalytic subunit cyclin-dependent kinase 1 (CDK1). With the exception of rodents, mammalian oocytes must synthesize CCNB1 de novo to form active MPF when meiosis is resumed. CCNB1 has not been detected in GV bovine [1] and porcine [2] oocytes, and microinjection of CCNB1 in the absence of protein synthesis is sufficient to induce GVBD in bovine oocytes [1]. MAPK, another important factor in meiotic regulation, is activated by mitogen activated protein kinase kinase (also known as MEK), which in turn is activated by MOS (Moloney murine sarcoma viral oncogene homolog). Whereas MOS production depends on de novo synthesis, MAPK and MEK are present in GV oocytes, but in an inactive state. Although MAPK activity within the oocyte is not required for meiotic resumption in farm animals [3–5], artificial activation of MAPK induces accelerated GV breakdown (GVBD) in bovine and porcine oocytes [5, 6] and is sufficient to induce GVBD in the absence of MPF activity [7–9]. Taken together, these data indicate that MPF and MAPK are key molecules regulating GVBD.

Many transcripts in oocytes are accumulated in a dormant state with short poly(A) tails; key proteins are produced by activation of these stored transcripts to orchestrate meiotic progression and early embryo cleavage. Activation of dormant mRNAs, including *CCNB1* and *MOS*, can be mediated by polyadenylation of their short poly(A) tails, which are polyadenylated during mammalian oocyte maturation [10–14], thus leading to their translation [11, 12, 15].

As well as being regulated by polyadenylation, *CCNB1* can form granules in the cytoplasm of immature mouse and zebrafish oocytes [16]. In zebrafish, these dormant RNA granules are disassembled following oocyte maturation to allow CCNB1 synthesis followed by GVBD, a process requiring actin depolymerization [16]. These findings suggest that release of *CCNB1* from granules plays an important role in the timing of *CCNB1* translation and subsequent GVBD.

The GV-arrested oocytes undergo cytoplasmic maturation within the ovary, but they resume meiosis spontaneously when removed from the inhibitory environment of the follicles. In an attempt to improve cytoplasmic maturation and enhance embryo development after in vitro fertilization (IVF), meiotic inhibitors have been used to prevent resumption of nuclear maturation of isolated oocytes. Cycloheximide (CHX), a protein synthesis inhibitor, has been widely used as a meiotic inhibitor because protein synthesis is critical for oocyte maturation [17, 18]. Meiotic arrest using CHX can improve developmental competence of porcine oocytes [19] but not of bovine oocytes [20–22], although live births have been reported after 24-h CHX arrest [22]. Interestingly, after CHX arrest, oocytes undergo accelerated GVBD, a phenomenon

[1]Supported by the University of Nottingham.
[2]Correspondence: Ramiro Alberio, Division of Animal Sciences, School of Biosciences, University of Nottingham, Sutton Bonington Campus, Loughborough LE12 5RD, United Kingdom.
E-mail: ramiro.alberio@nottingham.ac.uk
[3]Correspondence: Dylan Sweetman, Division of Animal Sciences, School of Biosciences, University of Nottingham, Sutton Bonington Campus, Loughborough LE12 5RD, United Kingdom.
E-mail: dylan.sweetman@nottingham.ac.uk
[4]Deceased.

Received: 16 June 2014.
First decision: 18 July 2014.
Accepted: 12 March 2015.

eISSN: 1529-7268 http://www.biolreprod.org
ISSN: 0006-3363

observed in sheep [17], cattle [23, 24], pigs [25], and goats [26]. However, the underlying mechanism of accelerated GVBD following meiotic arrest is unknown.

In the present study, we investigated the mechanism underlying accelerated meiotic progression in oocytes after CHX treatment and release from arrest. We hypothesized that whereas CHX prevents nuclear maturation, it does not prevent activation of meiotic resumption pathway(s) that may lead to the accumulation of key factors associated with meiotic progression in oocytes. We found that meiotic acceleration in ovine oocytes after release from CHX arrest was correlated with early accumulation of CCNB1 and increased MAPK phosphorylation. The mechanism underlying meiotic acceleration was not associated with mRNA polyadenylation or transcription of *CCNB1* or *MOS*. We show that stabilization of actin filaments during CHX arrest delays GVBD following release from arrest by delaying MPF activation, whereas disruption of actin filaments during arrest enhances the acceleration of GVBD following release. Our results support a model of actin depolymerization-mediated release of stored *CCNB1* during CHX arrest that becomes available to the translational machinery, thus leading to early translation of CCNB1 and accelerated meiotic progression after CHX withdrawal in oocytes from ungulates.

MATERIALS AND METHODS

Oocyte Recovery, CHX Treatment, and In Vitro Maturation of Oocytes

Ovine ovaries were collected from a local slaughter house and transported to the laboratory within 3 h in warm (30–35°C) PBS (160 mM NaCl, 3 mM KCl, 8 mM Na_2HPO_4, and 1 mM KH_2PO_4). Medium-sized (2–4 mm) follicles were aspirated using a needle and syringe. To the treatment group, CHX was added (final concentration, 5 μg/ml) to the follicular fluid during the aspiration process. Cumulus-oocyte complexes (COCs) with at least two layers of cumulus cells were selected for maturation using in vitro maturation (IVM) medium (bicarbonate-buffered M199 medium [Gibco] supplemented with 10% heat-inactivated fetal bovine serum [FBS], 0.05 U/ml of follicle-stimulating hormone/luteinizing hormone [Pluset], 1.0 μg/ml of 17β-estradiol, 50 μg/ml of gentamicin, 0.9 mM sodium pyruvate, and 0.1 mM cysteamine). For the treatment group, 5 μg/ml of CHX were added to the IVM medium. COCs were incubated in a humidified incubator at 39°C and 5% CO_2 in air. After the treatment period, COCs were washed three times in HEPES-buffered M199 and once in IVM medium and then matured in the same way as the control group. Cumulus expansion was assessed by measuring the area of COCs photographed before and after maturation using the SimplePCI software (Digital Pixel).

Assessment of Nuclear Maturation

Aceto-Orcein staining was carried out to determine the meiotic stages of oocytes. Cumulus cells were removed, and denuded oocytes were fixed in one part acetic acid and three parts ethanol for at least 24 h at room temperature. Fixed oocytes were stained in Aceto-Orcein stain solution (1% orcein and 45% acetic acid) for 10 min at room temperature. Oocytes were mounted and slides observed under phase-contrast microscopy at 1000× magnification.

IVF, Parthenogenesis, and Somatic Cell Nuclear Transfer

For IVF, a frozen ram semen pellet was thawed and incubated in capacitation medium (0.33 mM sodium pyruvate, 1.0 mM L-glutamine, 4.0 mM sodium bicarbonate, 21 mM HEPES, 3.35 mM sodium lactate, 108 mM sodium chloride, 7.2 mM potassium chloride, 1.2 mM potassium phosphate monobasic, 1.7 mM calcium chloride, 0.49 mM magnesium chloride, 2.4 mM glucose, 0.23 mM phenol red, 50 U/ml of penicillin, and 50 ng/ml of streptomycin; pH 7.4 and 270–290 mOsm) for 1 h at 39°C. Motile sperm were collected from the supernatant, centrifuged at 850 × *g* for 10 min at room temperature, and resuspended in a small volume of IVF medium (2% FBS, 1.0 mM sodium pyruvate, 1.0 mM L-glutamine, 25 mM sodium bicarbonate, 10 mM sodium lactate, 108 mM sodium chloride, 7.2 mM potassium chloride, 1.2 mM potassium phosphate monobasic, 3.4 mM calcium chloride, 0.49 mM magnesium chloride, 1.4 mM phenol red, 50 U/ml of penicillin, and 50 ng/ml of streptomycin; pH 7.9 and 270–290 mOsm). Matured COCs were incubated with 5 000 000 sperm/ml in IVF medium for 20 h in a humidified incubator at 39°C and 5% CO_2 in air. Presumptive zygotes were rinsed and cultured at 39°C with 5% CO_2 and 5% O_2 in synthetic oviduct fluid (SOF; 7.3 mM sodium pyruvate, 0.20 mM L-glutamine, 25 mM sodium bicarbonate, 5.4 mM sodium lactate [syrup], 108 mM sodium chloride, 7.2 mM potassium chloride, 1.2 mM potassium phosphate monobasic, 1.8 mM calcium chloride, 1.5 mM magnesium chloride, 0.34 mM trisodium citrate, 2.8 mM *myo*-inositol, 10 μg/ml of phenol red, 0.1 mM essential and nonessential amino acids, and 4 mg/ml of free-fatty-acids bovine serum albumin; pH 7.4 and 270–290 mOsm). Culture medium was changed at Day 3.

Somatic cell nuclear transfer (SCNT) was carried out as previously described [27] with minor modifications. Briefly, COCs were denuded of cumulus cells at 14 h postmaturation (hpm) by treatment with hyaluronidase (0.9 mg/ml; Sigma) combined with repeated, gentle pipetting. Oocytes with extruding spindles at anaphase I/telophase I (AI/TI) were selected for enucleation. AI/TI oocytes were briefly incubated in 10 μg/ml of Hoechst 33342 and 7.5 μg/ml of cytochalasin B (Sigma) in IVM medium, and enucleations were carried out in calcium-free, HEPES-buffered SOF (hSOF) with 7.5 μg/ml of cytochalasin B using a micromanipulator. Enucleated oocytes were returned to IVM containing 10 mM caffeine for 6 h until cell transfer. Fetal fibroblast donor cells were synchronized in G_0 by serum starvation for at least 2 days before SCNT. One cell was transferred into the perivitelline space of each enucleated oocyte and fused with one AC pulse of 1 V for 5 sec and two DC pulses of 100 V for 15 μsec each in fusion medium (0.3 M mannitol and 0.1 mM magnesium sulfate; 280 mOsm). Reconstructed embryos were further cultured in IVM medium for 2 h to allow nuclear envelope breakdown of the donor nucleus. Embryos were then activated at 25–27 hpm in hSOF containing 5 μM calcium ionophore (A23187) and calcium ions for 5 min, then rinsed and incubated with 10 μg/ml of CHX and 7.5 μg/ml of cytochalasin B in SOF for 5 h at 39°C with 5% CO_2 and 5% O_2. Oocytes were then thoroughly rinsed and incubated in SOF.

For parthenogenesis, COCs were denuded from cumulus cells at 24 hpm and then activated as described for SCNT.

Western Blot Analysis

Oocytes were completely denuded of cumulus cells, thoroughly rinsed in PBS, and stored at −80°C in 2 μl of PBS until use. Oocytes were lysed by adding one volume of 2× Laemmli buffer (Bio-Rad Laboratories) supplemented with phosphatase inhibitors (5 mM sodium fluoride, 2 mM sodium vanadate, and 2 mM β-glycerophosphate), vortexed, and heated at 95°C for 10 min. Samples were loaded into a denaturing polyacrylamide gel (SDS-PAGE) with lanes of 1.5 mm in width. Protein samples were electrophoresed at 150 V for 70 min, and resolved proteins were transferred onto a polyvinylidene fluoride membrane (Bio-Rad Laboratories) at 70 V for 3 h in transfer buffer (25 mM Tris, 192 mM glycine, and 20% methanol; pH 8.3). After transfer, membranes were blocked in 5% nonfat milk in PBS supplemented with 0.1% Tween 20 (PBS-T) for 1 h at room temperature, followed by overnight incubation at 4°C with primary antibody rabbit anti-CCNB1 (1:1000; C-8831; Sigma) in blocking buffer. After several washes in PBS-T, membranes were incubated with secondary antibody enhanced chemiluminescence (ECL) anti-rabbit immunoglobulin G conjugated to horseradish peroxidase (HRP; 1:30 000; NA934; Amersham Biosciences, GE Healthcare) in blocking buffer for 1 h at room temperature. The membrane was then washed six times for 5 min each time with PBS-T and treated with Amersham ECL Prime Western Blotting Detection Reagent (GE Healthcare). The chemiluminescence signal was developed with Hyperfilms ECL (Amersham). After washing, membranes were reprobed with rabbit anti-phospho-p44/42 MAPK antibody (1:2000; 9101; Cell Signaling Technology) in blocking buffer with a 2-h incubation at room temperature. Following signal detection, membranes were reprobed for the housekeeping protein α-tubulin using mouse monoclonal antibody anti-tubulin (1:2000; T5168; Sigma), followed by anti-mouse secondary antibody conjugated to HRP (1:10 000; SA1-100; Thermo Scientific) in blocking buffer. For total MAPK, membranes were stripped mildly, blocked, and incubated with anti-ERK1/2 antibody (1:2000; 9102; Cell Signaling Technology). Densitometric analysis of blots was carried out with ImageJ software (National Institutes of Health).

RNA-Ligation Polyadenylation Test

The RNA-ligation polyadenylation assay was used to compare the relative length of the poly(A) tail as previously described [28]. Briefly, total RNA was extracted from 30–50 oocytes using the Absolutely RNA Nanoprep kit (Agilent Technologies) and treated with DNase following the manufacturer's instructions. A modified anchor oligo (5′-P-GGTCACCTTGATCTGAAGC-NH_2-3′) was ligated to total RNA followed by cDNA synthesis with SuperScript III Reverse Transcriptase (Invitrogen) using the PAT-R1 primer (5′-GCTTCAGAT CAAGGTGACCTTTTT-3′). The QIAGEN Fast Cycling PCR Kit (Qiagen) was used to amplify target cDNA in 40 cycles of 96°C for 10 sec, 62°C for 10 sec,

and 68°C for 30 sec using the PAT-R1 reverse primer and the following forward gene specific primers (5′ to 3′): *CCNB1*, ggctgtggcaaaggtgtaac; *MOS*, ctctatgccgtggtggccta; and *GDF9* (growth differentiation factor 9), gtcctggccagtg taaatgc. PCR products were resolved in 1.5%–3% agarose gels prestained with ethidium bromide.

Quantitative RT-PCR

For gene expression analysis, quantitative RT-PCR (qRT-PCR) was carried out as previously described [29]. Briefly, total RNA was extracted from oocytes and converted to cDNA as described above. PCR reactions were performed on a LightCycler 480 (Roche Diagnostics) using 20-μl reactions containing 10 μl of FastStart SYBR Green Master Mix (Roche Diagnostics), 300 nM of each primer, and 1 μl of cDNA template. The thermal cycler program included a preincubation of 10 min at 95°C, followed by 45 cycles at 95°C for 20 sec, 62°C for 20 sec, and 72°C for 20 sec, with single fluorescence acquisition. Melting curves were performed to ensure gene-specific products. GAPDH was used as a reference gene for normalization, and relative transcript levels were calculated by the $\Delta\Delta C_T$ method. Primer pair sequences were as follows (5′ to 3′): *CCNB1,* gattggagaggttgatgttgag and aggtaatgctgtagagttggtg; *MOS*, gggcaa catcaccttgcacca and cgctgaccacgtctagggagta; *GDF9*, attagccttgattctctgccttctag and gtgtctcccacctaaatggttcag; and *GAPDH* (glyceraldehyde-3-phosphate dehydrogenase), gttccacggcacagtcaagg and actcagcaccagcatcaccc (sequences are forward and reverse, respectively).

Kinase Assay

The MPF activity was measured using histone H1 as in vitro substrate. Groups of 20 oocytes frozen in 5 μl were lysed by three cycles of thawing and freezing on dry ice. The kinase reaction was started by mixing 5 μl of PBS oocyte lysate with 5 μl of kinase assay buffer (45 mM β-glycerophosphate [pH 7.3], 20 mM MOPS [3-(N-morpholino)propansulfonic acid], 12 mM $MgCl_2$, 12 mM ethyleneglycol-tetra-acetic acid, 0.1 mM ethylenediaminetetra-acetic acid, 2 mM Na_3VO_4, 10 mM NaF, 2 mM dithiothreitol [DTT], 2 mM PMSF, 2 mM benzamidine, 20 μg/ml of leupeptin, 20 μg/ml of pepstatin, 20 μg/ml of aprotinin, 1 mg/ml of histone H1, 4 μM protein kinase A-inhibiting peptide [Santa Cruz Biotechnology], 4 μM protein kinase C-inhibiting peptide [Promega], and 0.5 μCi [34 μM] of [γ-^{32}P]ATP [Amersham Pharmacia Biotech]). The mixtures were incubated at 37°C for 45 min. The reaction was stopped by adding 10 μl of ice-cold 2× SDS sample buffer (125 mM Tris-HCl [pH 6.8], 200 mM DTT, 4% [w/v] SDS, 0.1% [w/v] bromophenol blue, and 20% [w/v] glycerol). The samples were then boiled for 4–5 min, and the substrates were separated by SDS-PAGE with 15% gels using a Mini-PROTEAN II Dual Slab Cell (Bio-Rad Laboratories) at a constant 150 V for 1.5 h. Gels were dried onto 3-mm filters for 1 h at 60°C and exposed to phosphor-screens (Kodak; Amersham Pharmacia Biotech). Kinase activity was quantified using ImageJ software.

Jasplakinolide and Cytochalasin B Treatments

To stabilize actin filaments during CHX arrest, oocytes were incubated with 5 μg/ml of CHX and 20 μM Jasplakinolide (Jasp; Millipore) in IVM medium. To destabilize actin filaments during CHX arrest, oocytes were incubated with 5 μg/ml of cytochalasin B and CHX in IVM medium. After treatment, oocytes were then washed and in vitro matured. All three treatment groups contained the same concentration of dimethyl sulfoxide (1%), the solvent in which Jasp was dissolved at a stock concentration of 1 mM.

Statistical Analysis

Student *t*-test or one-way ANOVA followed by Tukey multiple-comparison test were carried out for Figure 1 (GraphPad Prism, version 6.00; GraphPad Software). The differences in the proportions of oocytes undergoing GVBD after treatments groups were examined by analysis of deviance using generalized linear models assuming binomial errors and with logit link functions using GenStat (VSN international, release 11.1). Data are presented as the predicted back-transformed mean ± SEM.

RESULTS

Developmental Competence of CHX-Arrested Ovine Oocytes

Previous studies have reported inconsistent developmental outcomes of bovine and porcine CHX-treated oocytes [19–22]. In the present study, we characterized the developmental competence of CHX-arrested ovine oocytes by investigating meiotic progression after release, cumulus expansion, and blastocyst development after parthenogenesis, SCNT, and IVF.

First, we carried out a dose-response experiment to determine the minimal CHX concentration required to arrest ovine oocytes at the GV stage. A CHX concentration of 5 μg/ml was 95% effective in arresting oocytes at the GV stage and was therefore chosen for all subsequent experiments (Fig. 1, A and B). We found that after 24-h CHX arrest, 95% of released oocytes had undergone GVBD at 3 hpm, whereas in control oocytes, only 2% had undergone GVBD at 3 hpm (Fig. 1C). Accelerated GVBD was also observed after release from a shorter, 6-h arrest period, with 90% of oocytes versus 40% of controls having undergone GVBD at 5 hpm ($P = 0.02$) (Fig. 1D). Meiotic acceleration was maintained at 15 hpm, at which time 87% of oocytes released from CHX arrest had progressed beyond metaphase I (72% AI and 15% metaphase II [MII]) compared to 35% of nontreated oocytes (33% AI and 2% MII; $P = 0.01$) (Fig. 1D). By 22 h, nearly all oocytes in both groups had reached MII (Fig. 1D).

We then asked whether CHX-treated oocytes were developmentally competent. We first investigated the ability of COCs to undergo cumulus expansion after release from CHX arrest (Fig. 1E) by measuring the area of COCs before and after maturation. COCs incubated in CHX for 6, 12, and 24 h did not undergo cumulus expansion before CHX removal. Interestingly, the length of CHX treatment was inversely correlated with the capacity of COCs to undergo cumulus expansion after release from CHX arrest. A reduction of 13%, 30%, and 43% of cumulus expansion was observed for COCs treated with CHX for 6, 12, and 24 h, respectively, before IVM for 24 h (Fig. 1F, left). Nonetheless, all four COC groups reached MII at a high rate as assessed by polar body extrusion (80–90%) (Fig. 1F, right).

Next, we assessed the effects of CHX treatment on preimplantation development. We preincubated oocytes with CHX for 6 or 24 h (nontreated control oocytes were matured immediately after collection) and, after washing CHX away to allow maturation, performed parthenogenesis, SCNT, and IVF. We then assessed developmental competence by measuring cleavage rates and blastocyst development. After 24 h of CHX treatment followed by parthenogenesis, we observed a significant decrease in cleavage (29/51 vs. 52/52 of control embryos) and blastocyst formation (12/51 vs. 35/52 of control embryos) (Fig. 1G). The 24-h treatment with CHX followed by SCNT also produced reduced cleavage (78/104 vs. 106/112 of control embryos) and blastocyst formation (10/104 vs. 55/112 of control embryos) (Fig. 1H). Treatment with CHX for 6 h gave intermediate results following either parthenogenesis (cleavage of 41/45 and blastocyst formation of 24/45) or SCNT (cleavage of 109/121 and blastocyst formation of 39/121) (Fig. 1, G and H). Following IVF, no significant differences were observed in cleavage after either 6 or 24 h of CHX treatment compared to control oocytes, but blastocyst development was reduced in the 24-h CHX group (58/294) compared to the 6-h CHX group (119/273) and the control group (94/268) (Fig. 1I).

Increased Accumulation of CCNB1 and pMAPK after CHX Arrest

Germinal vesicle breakdown is accompanied by increases in CCNB1 synthesis and phosphorylation of MAPK. Therefore, we hypothesized that increased levels of these proteins mediated accelerated GVBD in CHX-treated oocytes. We compared the protein levels of CCNB1 and pMAPK between control and CHX-treated oocytes. At 6 h after release, we

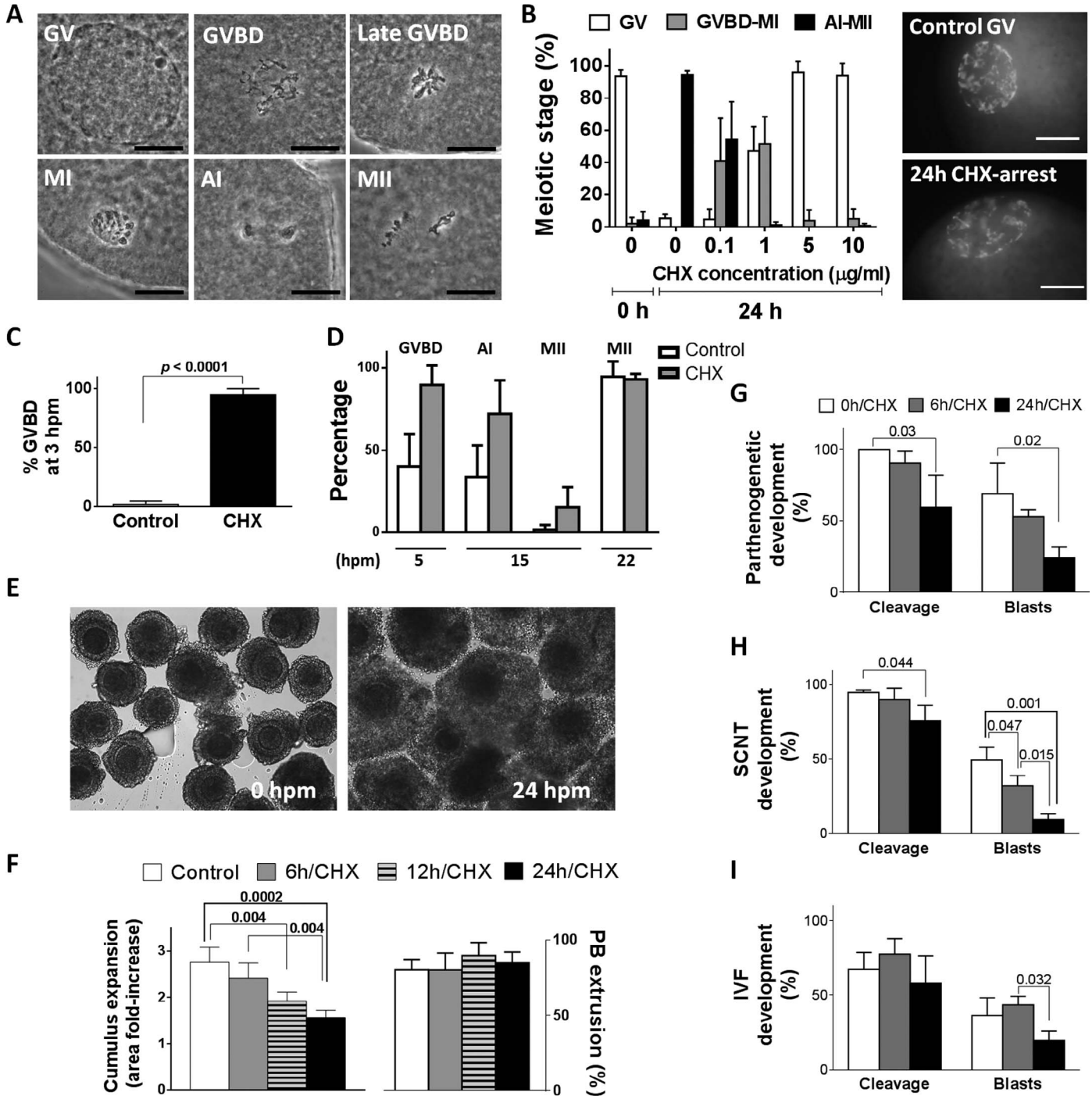

FIG. 1. Ovine oocytes released from CHX arrest undergo GVBD acceleration and have lower developmental competence. **A**) Representative meiotic stages assessed by Aceto-Orcein staining. **B**) Meiotic structures observed in oocytes cultured under different CHX concentrations (**left**) and 4′,6-diamidino-2-phenylindole staining of oocytes at the 0-h culture (control GV) or after 24 h in CHX (**right**). **C**) GVBD after 3-h release from CHX (arrested for 24 h) versus control oocytes at 3 hpm. **D**) Meiotic progression after 5, 15, and 22 h of maturation of oocytes released from CHX (arrested for 6 h) versus nontreated oocytes. **E**) Ovine COCs before maturation (0 hpm) and after 24 h of maturation (same magnification, ×100). **F**) Cumulus expansion after meiotic arrest with CHX (6, 12, or 24 h) and released for 24 h. Fold-increase in cumulus expansion (**left**) as well as polar body extrusion (**right**) were determined. **G**–**I**) CHX-arrested oocytes (treated for 6 and 24 h) were released after treatment, in vitro matured, and used for parthenogenesis (**G**), SCNT (**H**), or IVF (**I**). Cleavage was determined after 3 days of development, whereas blastocysts developed from activated/fertilized oocytes (blasts) were determined at Day 7. Error bars indicate the SD of three independent experiments. The *P*-values of significantly differing ($P < 0.05$) groups are presented. Bar = 20 μm.

observed a 3-fold increase in CCNB1 levels and an 18-fold increase in pMAPK levels compared to control oocytes matured for 6 h (Fig. 2). The results also show that changes in pMAPK are associated with phosphorylation rather than increased total MAPK levels.

Polyadenylation and Transcription of CCNB1 *and* MOS *Are Unchanged During CHX Treatment*

One possible explanation for the increased translation of CCNB1 and phosphorylation of MAPK in CHX-treated

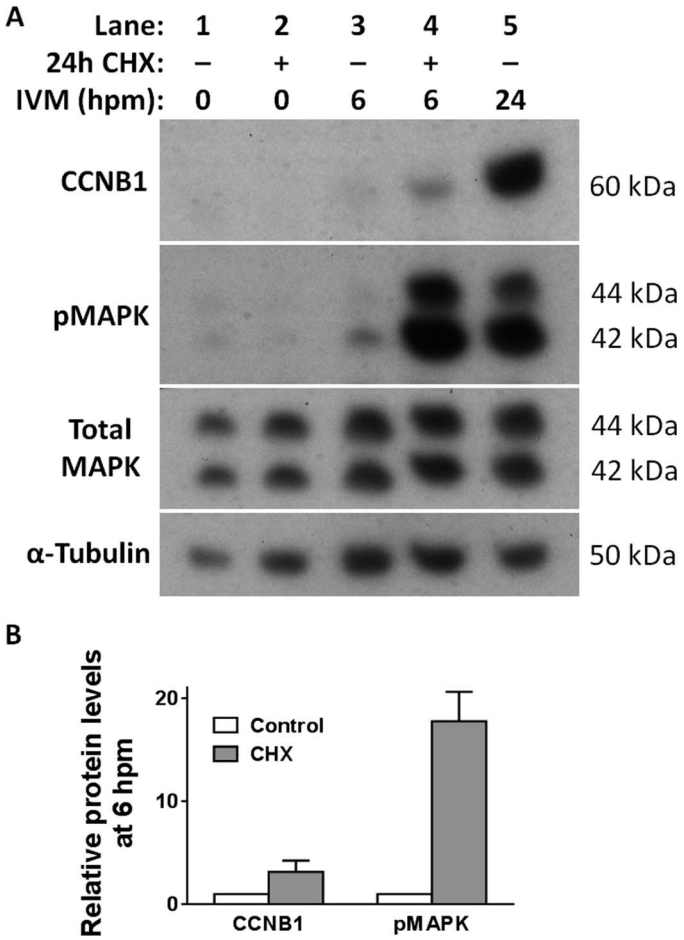

FIG. 2. Premature accumulation of CCNB1 and pMAPK in oocytes released from CHX arrest. **A**) Protein levels as determined by Western blot analysis of CCNB1 and pMAPK in 24-h CHX-arrested oocytes (lane 2) and released oocytes after 6 h of IVM (lane 4) as well as in nontreated control oocytes before IVM (lane 1) and after 6 h of IVM (lane 3); Matured (24-h) oocytes were included as positive controls (lane 5). From 80 to 120 oocytes were loaded per lane, and alpha-tubulin was used as a loading control. **B**) Densitometric analysis of Western blots at 6 hpm after tubulin normalization showing relative protein levels of CCNB1 and pMAPK in oocytes released from CHX arrest versus controls. Error bars indicate the range of two independent biological replicates.

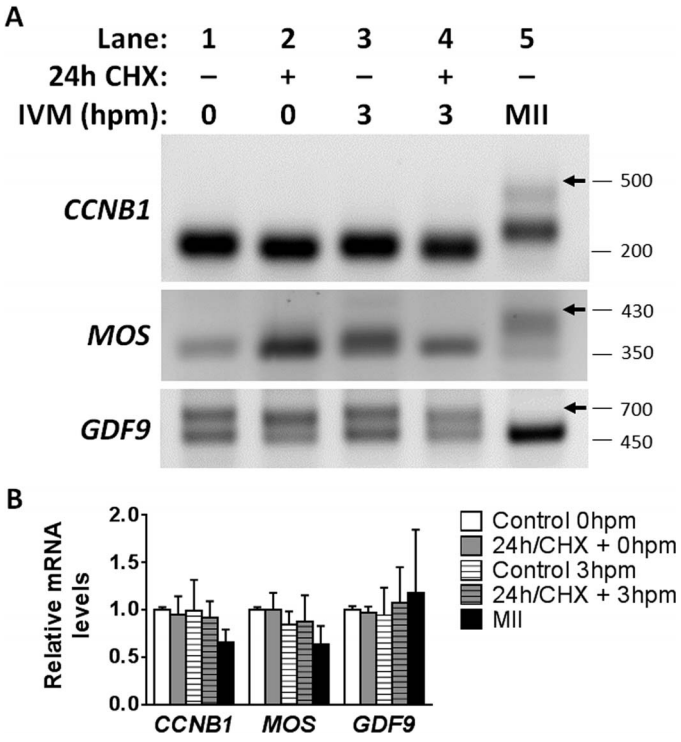

FIG. 3. Poly(A) tail length and levels of *CCNB1*, *MOS*, and *GDF9* mRNA are unchanged in CHX-treated ovine oocytes. **A**) RL-PAT analysis of control oocytes matured for 0 h (lane 1), 3 h (lane 3), and 24 h (MII; lane 5) as well as CHX-treated (24-h) oocytes before release (lane 2) or after release and 3 h of maturation (lane 4). A representative gel of two biological replicates is shown. Pictures are color-inverted for display purposes. Sizes are indicated in base pairs; arrows point to polyadenylated mRNA. **B**) Relative transcript levels determined by qRT-PCR. Samples were treated and matured as described in **A**. Error bars represent the SD of three biological replicates.

oocytes is that polyadenylation of *CCNB1* and *MOS* is initiated during CHX treatment. To test this possibility, we carried out an RL-PAT assay to compare the relative poly(A) tail length of these mRNAs in oocytes treated with CHX for 24 h. We found no polyadenylation in these transcripts before release from CHX arrest (Fig. 3A, lanes 1 and 2) and 3 h after release (Fig. 3A, lanes 3 and4), whereas extensive polyadenylation was detected in MII oocytes (Fig. 3A, lane 5). *GDF9*, which in contrast to *CCNB1* and *MOS* undergoes deadenylation during oocyte maturation, was also unaffected by CHX treatment (Fig. 3A).

As an alternative mechanism for early accumulation of our proteins of interest, we asked whether *CCNB1* and *MOS* mRNA levels increased during CHX treatment. We carried out qRT-PCR and found no statistically significant differences in the levels of these transcripts after 24-h CHX arrest and 3 h after release from arrest (Fig. 3B).

Actin Filament Destabilization During CHX Arrest Is Associated with Accelerated GVBD after Release

A recent study in zebrafish and mouse oocytes showed that *CCNB1* mRNA is stored in granules associated with actin filaments, which are released upon oocyte maturation [16]. To determine if premature release of actin-associated mRNAs could explain accelerated maturation following CHX treatment, we examined whether interfering with the stability of actin filaments during CHX arrest also affected GVBD. First, we assayed different concentrations (2.5, 5, 10, and 20 μM) of the actin filament-stabilizing agent Jasp in ovine oocytes treated for 6 h and found that the proportion of oocytes remaining at the GV stage was dose dependent (0%, 8%, 38%, and 85%, respectively). Then, we stabilized or destabilized actin filaments during CHX arrest with 20 μM Jasp or 5 μg/ml of cytochalasin B, respectively. After 6 h of treatment with CHX and either Jasp or cytochalasin B, oocytes were thoroughly rinsed and matured for 3 h. GVBD was delayed in the CHX/Jasp cotreatment group (39%, n = 156) compared to the CHX-alone group (66%, n = 168), whereas it was accelerated in the CHX/cytochalasin B cotreatment group (80%, n = 156) (Fig. 4A). Treatment of oocytes with Jasp alone did not prevent resumption of meiosis (69%, n = 65) (Fig. 4A). We also found that all oocytes following release from CHX/Jasp could progress beyond GVBD after 24 h of maturation (not shown), thus confirming that the GVBD delay in this group was due to actin filament stabilization and not toxic effects of the treatment. To confirm

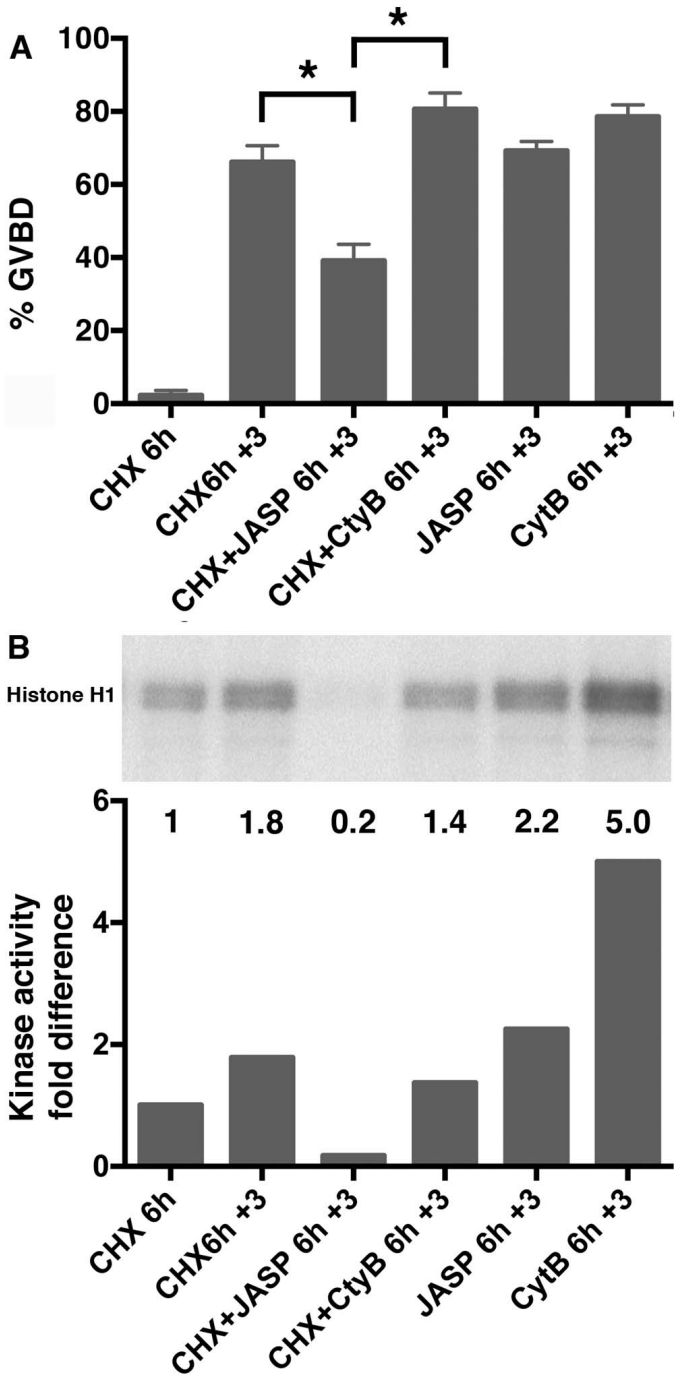

FIG. 4. Stabilization of actin filaments during CHX arrest prevent accelerated GVBD after release. **A**) Percentage of GVBD in oocytes treated with different compounds and matured for 3 h after release from CHX arrest. Error bars represent the SEM of four independent biological replicates. $*P < 0.01$. **B**) Histone H1 kinase activity in oocytes treated under different conditions. Quantification of band intensities is presented in the histogram. Values represent the fold-differences to the 6-h CHX-treated group, which was normalized to a value of one.

whether the effect on GVBD of Jasp in CHX-arrested oocytes was due to an effect on MPF activation, we performed a histone H1 kinase assay. The results show that MPF activity increased 1.8-fold in oocytes cultured for 3 h after CHX arrest compared to those collected after the 6 h of arrest (Fig. 4B). This increase correlates with the high proportion of GVBD observed (Fig. 4A). In contrast, oocytes treated with both CHX and Jasp showed very low levels of MPF activity. MPF levels in oocytes treated with both CHX and cytochalasin B were not different from those of the group released from CHX arrest. Oocytes cultured with Jasp or cytochalasin B alone showed increases in MPF. Taken together, these functional assays established an association between actin filament stability during meiotic arrest, MPF activation, and the kinetics of GVBD.

DISCUSSION

Our data support the hypothesis that early events normally associated with meiotic resumption occur during meiotic arrest with CHX, leading to premature accumulation of meiotic induction factors and subsequent acceleration of GVBD following release from arrest. We found that CCNB1 and pMAPK accumulate earlier in oocytes released from CHX arrest compared to nontreated oocytes. We showed that such accumulation is not mediated by polyadenylation or transcription of *CCNB1* and *MOS* during CHX arrest. Instead, our data suggest that stored *CCNB1* is released due to actin depolymerization during this period, thus facilitating translation of this ''free'' mRNA, leading to subsequent GVBD acceleration in released oocytes.

Because MPF and MAPK activities are key molecules mediating the kinetics of GVBD, we propose that the earlier accumulation of CCNB1 and pMAPK in oocytes released from CHX arrest is associated with GVBD acceleration. We show that CHX-arrested oocytes undergo a precocious activation of MPF, which correlates with the accelerated GVBD observed in this group.

A recent report provided an important insight regarding the possible mechanisms that might govern accelerated oocyte maturation after meiotic arrest. Kotani et al. [16] showed that dormant *CCNB1* mRNA forms granules that are associated with actin filaments and are released during oocyte maturation in zebrafish. They also found that preventing actin depolymerization with Jasp, which promotes actin filament polymerization and stability, prevents *CCNB1* RNA granule disassembly, CCNB1 synthesis, and GVBD in zebrafish oocytes. In contrast, treatment with cytochalasin B, an actin-depolymerizing agent, accelerated all of the above processes after induction of maturation [16]. Based on this, the authors suggested that actin depolymerization is involved in regulating the timing of CCNB1 synthesis and meiotic resumption in zebrafish oocytes. However, their study did not show whether similar events regulate meiotic resumption in mouse oocytes.

Our data extend these findings to large mammals and demonstrate a functional association between actin filament stability before maturation and subsequent kinetics of GVBD following maturation in ovine oocytes. We found that cotreatment of ovine oocytes with CHX and Jasp for 6 h significantly delays, but does not prevent, GVBD and reduces MPF activation following release from arrest compared to the CHX-alone group. This suggests that initiation of GVBD can also be triggered by alternative pathways (see below) and that MPF activation reinforces the process of meiotic progression. In contrast, cotreatment with CHX and cytochalasin B accentuated GVBD acceleration following release from these drugs. These findings in ovine oocytes are consistent with the role of actin depolymerization in regulating CCNB1 synthesis and GVBD described in zebrafish [16].

Based on these findings, we propose a model for the accelerated GVBD phenotype of CHX-treated mammalian oocytes (Fig. 5). In control oocytes, meiotic resumption initiates soon after removal from the ovarian follicle and

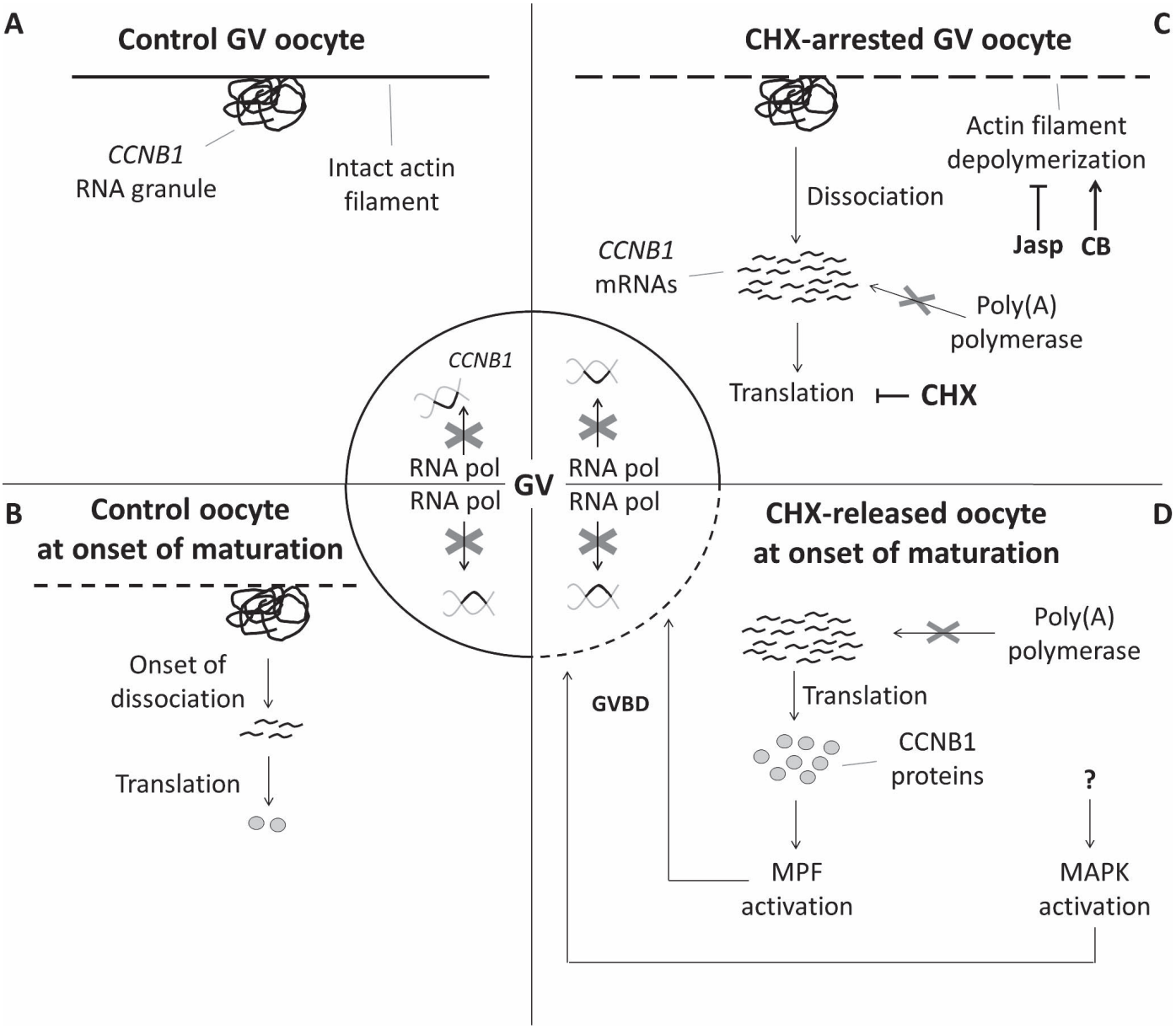

FIG. 5. Model of GVBD acceleration in CHX-treated mammalian oocytes. Neither polyadenylation nor transcription of *CCNB1* occurs during CHX arrest or during the onset of maturation. **A**) A GV oocyte contains *CCNB1* mRNA granules associated with intact actin filaments. **B**) This stored *CCNB1* mRNA starts to be released due to actin depolymerization at the onset of maturation. **C**) During CHX-induced meiotic arrest, depolymerization of actin filaments still occurs, thus inducing the release of stored *CCNB1* transcripts, but CHX inhibits their translation. **D**) Following CHX removal, the released stores of *CCNB1* mRNA facilitate its rapid translation, leading to precocious activation of MPF. MAPK activation is also accelerated, but the mechanism for this is unclear (see text). The premature activation of MPF and MAPK lead to accelerated GVBD. Counteracting actin depolymerization with Jasp during CHX arrest reduces the release of stored *CCNB1* mRNA and therefore delays the acceleration of GVBD following release from these drugs; the opposite outcome occurs during cotreatment with the actin depolymerizing agent cytochalasin B, followed by meiotic release.

results in a gradual release of stored *CCNB1* via actin filament depolymerization (Fig. 5, A and B). CHX-arrested oocytes still undergo actin filament depolymerization, causing the release of stored *CCNB1*, which becomes accessible to the translational machinery (Fig. 5C). Upon CHX removal, these transcripts are translated more readily, thus leading to earlier accumulation of CCNB1, precocious MPF activation, and acceleration of GVBD (Fig. 5D). In the present study, we also showed that actin depolymerization plays a role in regulating meiotic resumption during normal IVM in mammals because treatment of ovine oocytes with Jasp alone delayed GVBD. However, in contrast to zebrafish [16], Jasp cannot prevent GVBD in ovine oocytes, similar to the findings in mouse [30]. This discrepancy between species suggests that either mammalian oocytes require a much higher concentration of Jasp to prevent GVBD or that actin depolymerization plays a more important role in regulating GVBD in fish.

The mechanism underlying premature MAPK activation observed in oocytes released from CHX arrest has yet to be established. One possibility is that stored *MOS* behaves similarly to *CCNB1*, forming granules associated with actin that are released upon oocyte maturation to allow synthesis of MOS and activation of the MOS/MEK/MAPK signaling cascade. Consistent with this is the formation of *MOS* mRNA aggregates around the oocyte cortex, a region rich in ribonucleoproteins in mouse GV oocytes [31]. Furthermore,

increasing the pool of ''free'' *MOS* by microinjection of mRNA into bovine oocytes resulted in maximal MAPK activation and GVBD acceleration after only 6 h of maturation [6]. This phenotype is very similar to what we find in oocytes released from CHX arrest, consistent with the idea that ''free'' *MOS* is released from dormant stores during that arrest.

Our data do not support alternative explanations hypothesized for meiotic acceleration, including increased mRNA polyadenylation or transcription during CHX-induced arrest. This is consistent with previous reports in progesterone-stimulated *Xenopus* oocytes in which no polyadenylation was observed in the presence of CHX [32, 33]. Therefore, either protein synthesis, meiotic resumption, or both are necessary for polyadenylation of dormant mRNA. Interestingly, we found no increased levels of polyadenylation of *CCNB1* or *MOS* even after 3 h of release from arrest, demonstrating that polyadenylation is not accelerated and therefore cannot be the cause of increased levels of CCNB1 and pMAPK observed 6 h after release. Our data also rule out the possibility of increased transcription resulting in higher levels of *CCNB1* and *MOS* during CHX arrest because levels of these transcripts remained unchanged. This was expected as GV oocytes have low transcriptional activity before meiotic resumption [34, 35].

Some authors have reported chromatin condensation during CHX arrest [23] and proposed that MPF is partially activated during this period, thus partly explaining the accelerated GVBD following CHX release. However, another group failed to confirm these differences in chromatin configurations between control and CHX-arrested bovine GV oocytes [24]. Our data support this latter conclusion as we also failed to see chromatin condensation in either bovine (not shown) or ovine oocytes arrested with CHX (Fig. 1B).

Although the present study focused primarily on molecular events within the oocyte, cumulus cells also play a crucial role in regulating oocyte meiotic resumption. Upon removal of the COC from the inhibitory follicular environment, MAPK activation in cumulus cells leads to disruption of gap junction communications and subsequent decrease of the meiosis-inhibiting molecule cAMP within the oocyte as cumulus cells depends on these channels to maintain intraoocyte cAMP levels (for review, see [4, 36, 37]). It is possible that phosphorylation of MAPK in cumulus cells could occur during CHX treatment of COCs, as reported in mice [38]. Therefore, after CHX arrest, low cAMP levels in the oocyte would facilitate rapid resumption of meiosis. This additional mechanism contributing to meiotic acceleration of CHX-treated oocytes needs to be fully tested, including whether MAPK activation in cumulus cells still occurs in the absence of protein synthesis in large mammals, whether gap junctions are disrupted if it is, and finally, whether intraoocyte cAMP levels decrease during treatment. In addition, there could be various posttranslational modifications in the oocyte and cumulus cells induced upon removal of the COC from the follicle that are independent of protein synthesis.

In addition to accelerated meiotic progression, we found that oocytes released from CHX arrest undergo reduced cumulus expansion and have lower developmental competence, with all three phenotypes being accentuated after longer exposure to CHX. Impaired cumulus expansion has also been observed after release from MPF inhibitors in bovine oocytes [39]. These findings suggest that meiotic arrest induced with pharmacological agents can impair cumulus function. The correlation found between cumulus expansion and subsequent embryo development is consistent with previous results in porcine COCs [40]. Lower development to blastocysts has been consistently observed in bovine oocytes after 24-h arrest with CHX [20–22]. However, improved development was reported after a 12-h CHX treatment in porcine oocytes [18]. This discrepancy in developmental outcome might be a species-specific response to CHX. Nonetheless, shorter CHX treatments are compatible with development [20–22] (present study).

In summary, our findings support a model of actin depolymerization-mediated release of *CCNB1* stores during CHX arrest, which results in premature accumulation of CCNB1 and leads to meiotic acceleration following release from arrest in mammalian oocytes. Accelerated maturation in released oocytes appears to be caused by early meiotic resumption during CHX arrest. Thus, we suggest that if meiotic inhibitors are to be used to improve oocyte quality, it may be necessary to identify methods that prevent both accelerated meiotic progression and reduced cumulus expansion, which may compromise the developmental capacity of these oocytes.

ACKNOWLEDGMENT

We thank Cornelia de Moor for her guidance in the RL-PAT assay and Susan Liddell for her help with the kinase assays.

REFERENCES

1. Levesque JT, Sirard MA. Resumption of meiosis is initiated by the accumulation of cyclin B in bovine oocytes. Biol Reprod 1996; 55: 1427–1436.
2. Naito K, Hawkins C, Yamashita M, Nagahama Y, Aoki F, Kohmoto K, Toyoda Y, Moor RM. Association of $p34^{cdc2}$ and cyclin B1 during meiotic maturation in porcine oocytes. Dev Biol 1995; 168:627–634.
3. Gordo AC, He CL, Smith S, Fissore RA. Mitogen activated protein kinase plays a significant role in metaphase II arrest, spindle morphology, and maintenance of maturation promoting factor activity in bovine oocytes. Mol Reprod Dev 2001; 59:106–114.
4. Liang CG, Su YQ, Fan HY, Schatten H, Sun QY. Mechanisms regulating oocyte meiotic resumption: roles of mitogen-activated protein kinase. Mol Endocrinol 2007; 21:2037–2055.
5. Ohashi S, Naito K, Sugiura K, Iwamori N, Goto S, Naruoka H, Tojo H. Analyses of mitogen-activated protein kinase function in the maturation of porcine oocytes. Biol Reprod 2003; 68:604–609.
6. Fissore RA, He CL, Vande Woude GF. Potential role of mitogen-activated protein kinase during meiosis resumption in bovine oocytes. Biol Reprod 1996; 55:1261–1270.
7. de Vantery Arrighi C, Campana A, Schorderet-Slatkine S. A role for the MEK-MAPK pathway in okadaic acid-induced meiotic resumption of incompetent growing mouse oocytes. Biol Reprod 2000; 63:658–665.
8. Gavin AC, Cavadore JC, Schorderet-Slatkine S. Histone H1 kinase activity, germinal vesicle breakdown and M phase entry in mouse oocytes. J Cell Sci 1994; 107(pt 1):275–283.
9. Motlik J, Pavlok A, Kubelka M, Kalous J, Kalab P. Interplay between CDC2 kinase and MAP kinase pathway during maturation of mammalian oocytes. Theriogenology 1998; 49:461–469.
10. Gebauer F, Xu W, Cooper GM, Richter JD. Translational control by cytoplasmic polyadenylation of c-mos mRNA is necessary for oocyte maturation in the mouse. EMBO J 1994; 13:5712–5720.
11. Lazar S, Galiani D, Dekel N. cAMP-dependent PKA negatively regulates polyadenylation of c-*mos* mRNA in rat oocytes. Mol Endocrinol 2002; 16: 331–341.
12. Nishimura Y, Kano K, Naito K. Porcine CPEB1 is involved in cyclin B translation and meiotic resumption in porcine oocytes. Anim Sci J 2010; 81:444–452.
13. Tremblay K, Vigneault C, McGraw S, Sirard MA. Expression of cyclin B1 messenger RNA isoforms and initiation of cytoplasmic polyadenylation in the bovine oocyte. Biol Reprod 2005; 72:1037–1044.
14. Zhang DX, Cui XS, Kim NH. Molecular characterization and polyadenylation-regulated expression of cyclin B1 and Cdc2 in porcine oocytes and early parthenotes. Mol Reprod Dev 2010; 77:38–50.
15. Lazar S, Gershon E, Dekel N. Selective degradation of cyclin B1 mRNA in rat oocytes by RNA interference (RNAi). J Mol Endocrinol 2004; 33: 73–85.
16. Kotani T, Yasuda K, Ota R, Yamashita M. Cyclin B1 mRNA translation is

temporally controlled through formation and disassembly of RNA granules. J Cell Biol 2013; 202:1041–1055.
17. Moor RM, Crosby IM. Protein requirements for germinal vesicle breakdown in ovine oocytes. J Embryol Exp Morphol 1986; 94:207–220.
18. Motlik J, Rimkevicova Z. Combined effects of protein synthesis and phosphorylation inhibitors on maturation of mouse oocytes in vitro. Mol Reprod Dev 1990; 27:230–234.
19. Ye J, Campbell KH, Craigon J, Luck MR. Dynamic changes in meiotic progression and improvement of developmental competence of pig oocytes in vitro by follicle-stimulating hormone and cycloheximide. Biol Reprod 2005; 72:399–406.
20. Lonergan P, Fair T, Khatir H, Cesaroni G, Mermillod P. Effect of protein synthesis inhibition before or during in vitro maturation on subsequent development of bovine oocytes. Theriogenology 1998; 50:417–431.
21. Lonergan P, Khatir H, Carolan C, Mermillod P. Bovine blastocyst production in vitro after inhibition of oocyte meiotic resumption for 24 h. J Reprod Fertil 1997; 109:355–365.
22. Saeki K, Nagao Y, Kishi M, Nagai M. Developmental capacity of bovine oocytes following inhibition of meiotic resumption by cycloheximide or 6-dimethylaminopurine. Theriogenology 1997; 48:1161–1172.
23. Simon M, Jilek F, Fulka J Jr. Effect of cycloheximide upon maturation of bovine oocytes. Reprod Nutr Dev 1989; 29:533–540.
24. Tatemot H, Horiuchi T, Terada T. Effects of cycloheximide on chromatin condensations and germinal vesicle breakdown (GVBD) of cumulus-enclosed and denuded oocytes in cattle. Theriogenology 1994; 42: 1141–1148.
25. Kubelka M, Motik J, Fulka J Jr, Prochazka R, Rimkevicova Z, Fulka J. Time sequence of germinal vesicle breakdown in pig oocytes after cycloheximide and P-aminobenzamidine block. Gamete Res 1988; 19: 423–431.
26. Le Gal F, Gall L, De Smedt V. Changes in protein synthesis pattern during in vitro maturation of goat oocytes. Mol Reprod Dev 1992; 32:1–8.
27. Lee JH, Campbell KH. Effects of enucleation and caffeine on maturation-promoting factor (MPF) and mitogen-activated protein kinase (MAPK) activities in ovine oocytes used as recipient cytoplasts for nuclear transfer. Biol Reprod 2006; 74:691–698.
28. Rassa JC, Wilson GM, Brewer GA, Parks GD. Spacing constraints on reinitiation of paramyxovirus transcription: the gene end U tract acts as a spacer to separate gene end from gene start sites. Virology 2000; 274: 438–449.
29. Choi I, Lee JH, Fisher P, Campbell KH. Caffeine treatment of ovine cytoplasts regulates gene expression and foetal development of embryos produced by somatic cell nuclear transfer. Mol Reprod Dev 2010; 77: 876–887.
30. Terada Y, Simerly C, Schatten G. Microfilament stabilization by jasplakinolide arrests oocyte maturation, cortical granule exocytosis, sperm incorporation cone resorption, and cell-cycle progression, but not DNA replication, during fertilization in mice. Mol Reprod Dev 2000; 56: 89–98.
31. Flemr M, Ma J, Schultz RM, Svoboda P. P-body loss is concomitant with formation of a messenger RNA storage domain in mouse oocytes. Biol Reprod 2010; 82:1008–1017.
32. Ballantyne S, Daniel DL Jr, Wickens M. A dependent pathway of cytoplasmic polyadenylation reactions linked to cell cycle control by c-mos and CDK1 activation. Mol Biol Cell 1997; 8:1633–1648.
33. McGrew LL, Richter JD. Translational control by cytoplasmic polyadenylation during *Xenopus* oocyte maturation: characterization of cis and trans elements and regulation by cyclin/MPF. EMBO J 1990; 9: 3743–3751.
34. Fair T, Hyttel P, Greve T. Bovine oocyte diameter in relation to maturational competence and transcriptional activity. Mol Reprod Dev 1995; 42:437–442.
35. Fair T, Hyttel P, Greve T, Boland M. Nucleus structure and transcriptional activity in relation to oocyte diameter in cattle. Mol Reprod Dev 1996; 43: 503–512.
36. Edry I, Sela-Abramovich S, Dekel N. Meiotic arrest of oocytes depends on cell-to-cell communication in the ovarian follicle. Mol Cell Endocrinol 2006; 252:102–106.
37. Gilchrist RB. Recent insights into oocyte-follicle cell interactions provide opportunities for the development of new approaches to in vitro maturation. Reprod Fertil Dev 2011; 23:23–31.
38. Fan HY, Huo LJ, Chen DY, Schatten H, Sun QY. Protein kinase C and mitogen-activated protein kinase cascade in mouse cumulus cells: cross talk and effect on meiotic resumption of oocyte. Biol Reprod 2004; 70: 1178–1187.
39. Lonergan P, Faerge I, Hyttel PM, Boland M, Fair T. Ultrastructural modifications in bovine oocytes maintained in meiotic arrest in vitro using roscovitine or butyrolactone. Mol Reprod Dev 2003; 64:369–378.
40. Qian Y, Shi WQ, Ding JT, Sha JH, Fan BQ. Predictive value of the area of expanded cumulus mass on development of porcine oocytes matured and fertilized in vitro. J Reprod Dev 2003; 49:167–174.